Cement and Concrete Research 173 (2023) 107302

Contents lists available at ScienceDirect

Cement and Concrete Research

journal homepage: www.elsevier.com/locate/cemconres

Effect of hydroxide, carbonate, and sulphate anions on the β-dicalcium silicate hydration rate

Muhammad Jawad Ahmed *, Kim Lambrechts, Xuan Ling, Katrin Schollbach, H.J.H. Brouwers

Department of Built Environment, Eindhoven University of Technology, Eindhoven, the Netherlands

ARTICLE INFO

Keywords:
β-Dicalcium silicate
In-situ conductivity
Anions
Hydration degree
Dissolution-precipitation

ABSTRACT

The effect of fixed (0.8 M) Na^+ balanced by either OH^-, SO_4^{2-}, and CO_3^{2-} anions on β-dicalcium silicate (C_2S) reactivity is investigated. The exothermic reaction of varying water-to-solid ratios and chemical activation is monitored. Subsequently, the hydration products are characterized via FTIR, TG/DTG, QXRD, and SEM analysis. The findings showed that the carbonate ions expedited the reactivity up to 55% at 1–7 days due to the simultaneous precipitation of calcium silicate hydrate (C-S-H) and calcite. At 7–28 days, the lack of transportable cations between the solid surface and solution impeded further hydration, as confirmed by *in-situ* pH and conductivity measurements. The sulphate ions accelerated the reactivity only upon calcium sulphate dissolution at high pH. The hydroxide ions decelerated the hydration due to the earlier precipitation of portlandite than C-S-H. Overall, the β-C_2S reaction with water exhibited the highest hydration degree (~67%) after 28 days of hydration.

1. Introduction

Dicalcium silicate (C_2S) is an important constituent of belite clinker (40–60%), belite calcium sulfoaluminate cement (25–50%), basic Oxygen furnace steel slag (30–50%), and ordinary Portland cement (OPC, 10–15%), where it exists in the form of β-C_2S polymorph, stabilized at room temperature due to presence of impurities [1–5]. Belite-rich binders are more sustainable than OPC because less calcite is needed to produce them as the enthalpy of formation for alite is higher than belite (~1810 kJ/kg, ~1350 kJ/kg, respectively), by lowering the kiln operating temperature (~1200–1350 °C) and the associated CO_2 emissions [6]. However, the main drawback that restricts the application of belite cement is the low reactivity of β-C_2S leading to slow strength development [7]. The material admixture especially NaOH, KOH, C-S-H seeds, and commercial oxide nanoparticles, etc. is reported to accelerate the hydration of belite cement where the excess cumulative heat release is attributed to the β-C_2S reactivity [2,6,8]. Thus, a systematic understanding of the β-C_2S hydration via chemical activation is a prerequisite for its technical application.

Several strategies have been reported to improve the C_2S hydration by mechanical grinding, mineralizers, or dopants (NaF, SO_3, B_2O_3, etc.) and chemical activators such as alkali oxides, salts as well as calcium silicate hydrate (C-S-H) seeds [9–12]. Chemical activation particularly NaOH, KOH, Na_2CO_3, and K_2CO_3, etc. is acknowledged to accelerate the C_2S hydration due to the interaction of calcium silicate hydrate (C-S-H) with soluble alkali oxides [7,13–16]. β-C_2S reactivity in NaOH and KOH hydration mediums is reported to increase both the hydration degree alongside associated early strength development [13,17,18]. Especially, a high concentration of 5 M KOH could significantly accelerate the β-C_2S reactivity, while it was demonstrated that low concentrations of NaOH slow down the dissolution of β-C_2S [7,19]. The improved hydraulic properties of β-C_2S in the KOH environment are attributed to the larger ionic radius and electronegativity of potassium cation compared to sodium ion [18,20]. These differences in ionic properties would give different interactions with the C-S-H formation and associated mechanical properties. Moreover, the addition of carbonate solutions was reported to shorten the induction period alongside improved hydraulic activity of C_2S, especially at low $NaHCO_3$ concentrations which were more effective than KOH [18]. Subsequently, a 0.28 M Na_2SO_4-activated C_2S exhibited a better 28-day mechanical strength than Na_2CO_3 without significant change in hydraulic activity [21–23]. The emphasis of these studies lies more on the role of cation interaction (Na^+, K^+) with C-S-H, especially the Ca/Si ratio, C-(Na/K)-S-H, and the degree of silicate chain polymerization. But the presence of anions equally impacts the reaction kinetics, particularly the C-S-H dissolution-precipitation reaction.

Very few studies have investigated the effect of the anions on tuning the β-C_2S reactivity [21]. Especially information about the β-C_2S dissolution-precipitation as well as its correlation with solution ionic

* Corresponding author.
E-mail address: m.ahmed@tue.nl (M.J. Ahmed).

https://doi.org/10.1016/j.cemconres.2023.107302
Received 13 April 2023; Received in revised form 19 July 2023; Accepted 6 August 2023
Available online 18 August 2023

strength and hydration degree over time is missing. In addition to that, the non-systematic concentrations of the activators reported in the literature make it difficult to compare the effect of cations and anions in the hydration process [18,24–26]. If undersaturation is the leading cause of the C_2S dissolution, then the anions also play a vital role in dictating the C-S-H precipitation alongside cations [27] as it has been often ignored. Therefore, a systematic approach is desired to understand the contribution of anions, pH, and ionic strength to comprehend the hydration rate at ambient conditions. To the author's best knowledge, there is no systematic study reported where the amount of activator is adjusted to have fixed moles of sodium cations containing hydroxide, carbonate, and sulphate anions for β-C_2S chemical activation.

For this purpose, pure β-C_2S was synthesized at 1200 °C via the Pechini method. The synthesis method and calcination condition are chosen to attain lime-free C_2S. To study the effect of anions on β-C_2S activation, the molarity of sodium ion is fixed to 0.8 M to have comparable Na^+ concentration in all samples. The effect of dissolution degree on the β-C_2S reactivity is investigated to promote the forward direction dissolution reaction at ambient conditions by using the water to the solid (w/s) ratios between 0.5 and 1.6. Moreover, the order of hydration product formation and degree of hydration (DOH) is correlated with the anionic effect via the bonding system, thermal, mineralogical, and microstructural analysis over 28 days of hydration. Finally, the heat release is correlated with the concentration of hydroxyl ions alongside the ionic strength of the hydrating media at an early stage (1–5 days) via *in-situ* pH and conductivity measurements to understand the β-C_2S dissolution-precipitation reaction events.

2. Materials and methods

$Ca(NO_3)_2{\cdot}4H_2O$ (Sigma-Aldrich, CAS: 13477-34-4), colloidal SiO_2 (40 wt%, LUDOX® AS-40, Sigma-Aldrich, CAS: 7631-86-9), TEOS/Si $(OC_2H_5)_4$ (Sigma-Aldrich, CAS: 78-10-4), Citric acid monohydrate (VWR, CAS: 5949-29-1), ethylene glycol (VWR, CAS: 107-21-1), 65% HNO_3 (Sigma-Aldrich, CAS:7697-37-2), ethanol (Sigma-Aldrich, CAS:64-17-5) were used as received. The reagents were added in the stoichiometric ratios 2:1 Ca/Si corresponding to the synthesis of C_2S. C_2S has been synthesized via the Pechini method by calcining intermediate charred gel at 1200 °C. A detailed synthesis method can be studied elsewhere [28].

Alkali salts NaOH (Merck, CAS: 1310-73-2), Na_2CO_3 (Sigma-Aldrich CAS: 497-19-8), and Na_2SO_4 (Merck, CAS: 7757-82-6) were dissolved in deionized water (DI). The resulting solutions are directly used as hydration media in this study. Moreover, the $CaCO_3$ from Sigma-Aldrich (CAS: 471-43-1, ≥99.0%) is used to study the filler effect.

2.1. Hydration studies

A fixed molar concentration of sodium cations such as 0.8 M NaOH, 0.4 M Na_2CO_3, and 0.4 M Na_2SO_4 is used as alkali activators for β-C_2S. Isothermal calorimetric measurements were conducted in TAM AIR isothermal calorimetric device at 20 ± 0.5 °C for 14 days. Predetermined amounts of the C_2S were added to the vials. After acclimatization of the materials and hydration media to room temperature, the sample was mixed *ex situ*. After the designated time, the hydration was stopped by solvent exchange method (immersing in isopropanol followed by diethyl ether washing) and samples are labeled as shown in Table 1.

In-situ pH and conductivity measurements of the hydrating samples were executed in a climate-controlled room, which is kept at 20 ± 0.5 °C with 60% humidity. After acclimatization of the solutions the conductivity probe, the Greisinger-GMH 3431, and the Voltcraft -PE-03 pH probe were calibrated. The hydration media was stirred by hand upon insertion of probes and data logging with a 7.5-minute interval was started. To prevent water evaporation the beaker was sealed with parafilm and tape. The pH and conductivity measurements were performed with a 1.6 w/s ratio. As the excess water increased the volume, it ensured the probes were in full contact with the system. The starting pH values of the alkali activators are presented in Table 1.

2.2. Characterization techniques

X-ray powder diffractograms were acquired using a Bruker D2 diffractometer with an X-ray Co radiation X-ray source. The instrument has a fixed divergence slit with an opening of 0.5° and 0.04 rad Soller slits. Reflections were measured between 5° and 90° 2 Theta (θ) with a step size of 0.02°. The cured (7, 14, and 28 days old) samples were subjected to hydration stoppage via solvent exchange (Isopropanol, Diethyl ether) method. All samples for qualitative and quantitative analysis were prepared via back-loading. The mineral phases were identified with X'Pert Highscore Plus 2.2 employing the ICDD PDF-2 database. For QXRD (quantitative X-ray diffraction), 10 wt% silicon was added to the hydrated samples. The samples were homogeneously mixed utilizing a McCrone micronizing mill. Quantification was done with TOPAS 4.2 software from Bruker. All crystal structures for quantification were obtained from the ICSD database. The error values given in the results are calculated by TOPAS 4.2. The quantitative X-ray diffraction (QXRD) analysis of synthesized C_2S has been shown in Table 2. C_2S synthesized by the Pechini method contains a high amount of β-C_2S (~83 wt%) with no free lime alongside ~8 wt% γ-C_2S (Table 2, see Fig. S1 (a) for Rietveld plot) and a low amorphous content (~9 wt%).

To understand the impact of specific surface area (SSA) on the hydration kinetics, the nitrogen adsorption (Tristar II 3020 V1.03 series micrometer) at 77 K was measured using BET (Brunauer-Emmett-Teller) methods (Table 2).

TG (thermogravimetry) analysis was performed on the hydrated sample (hydration stopped via solvent exchange method [29]) via a Jupiter STA 449 F1 (Netzsch) with heating of 15 °C/min under an N_2 environment up to 1000 °C.

The IR spectra were measured with a Fourier Transform-Infrared spectrometer (FT-IR) from Perkin Elmer Frontier FTIR. The spectrometer was equipped with a diffuse reflectance device GladiATR. Forty scans are acquired with optical retardation of 0.25 cm and a resolution of 4 cm^{-1} from 400 to 4000 cm^{-1}.

Scanning Electron Microscopy (SEM) was performed for microstructure analysis using a Phenom Pro-X. The sample was prepared by spreading the hydrated powder sample (hydration stopped via solvent exchange method) on conductive carbon adhesive tapes followed by coating with gold with Qourum 150TS plus sputter coater. Micrographs were recorded using a backscattered electron detector (BSE) at 15 kV with a spot of four.

Table 1
Sample labeling of the hydration mediums at 20 ± 0.5 °C and 60% relative humidity.

Hydration mediums	C_2S + water	C_2S + 0.8 M NaOH solution	C_2S + 0.4 M Na_2CO_3 solution	C_2S + 0.4 M Na_2SO_4 solution
Sample label	Reference	0.8 M NaOH	0.4 M Na_2CO_3	0.4 M Na_2SO_4
pH	7.2	13.2	11.3	6.9

Table 2
QXRD of the C_2S synthesized at 1200 °C via the Pechini method with error values and specific surface area (SSA).

Mineral phases	β-C_2S	γ-C_2S	Quartz	Wollastonite 2-M	XRD-amorphous
Amount (wt %)	82.7 ± 0.2	8.0 ± 0.1	0.9 ± 0.1	0.1 ± 0.07	8.4 ± 1.2
BET-SSA (m^2/g)	0.85				

3. Results and discussion

3.1. Hydration behaviour in varying water-to-solid (w/s) ratio

The 14 days hydration behaviour of β-C_2S with water and 0.8 mol of Na^+ activators was monitored via isothermal calorimetry as shown in Fig. 1 (a, b). The heat flow is normalized by the mass of the sample. Two different w/s ratios (1.6 and 0.5) were investigated to understand the effect of dissolution degree on β-C_2S reactivity. The results for a w/s ratio of 1.6 indicated that the reference sample exhibited no significant exothermic heat of hydration. However, around ~96 h, a clear increase in the heat flow indicated C-S-H precipitation [30]. A heat flow pattern just like the reference was observed for 0.8 M NaOH as well as 0.4 M Na_2SO_4 samples. The addition of the same moles of sodium activator did not alter the exothermic heat of C_2S hydration till ~96 h except for the 0.4 M Na_2CO_3 sample. The exothermic heat pattern has conspicuous features of dissolution as well as an induction period followed by an acceleration and deceleration period featured in the 0.4 M Na_2CO_3

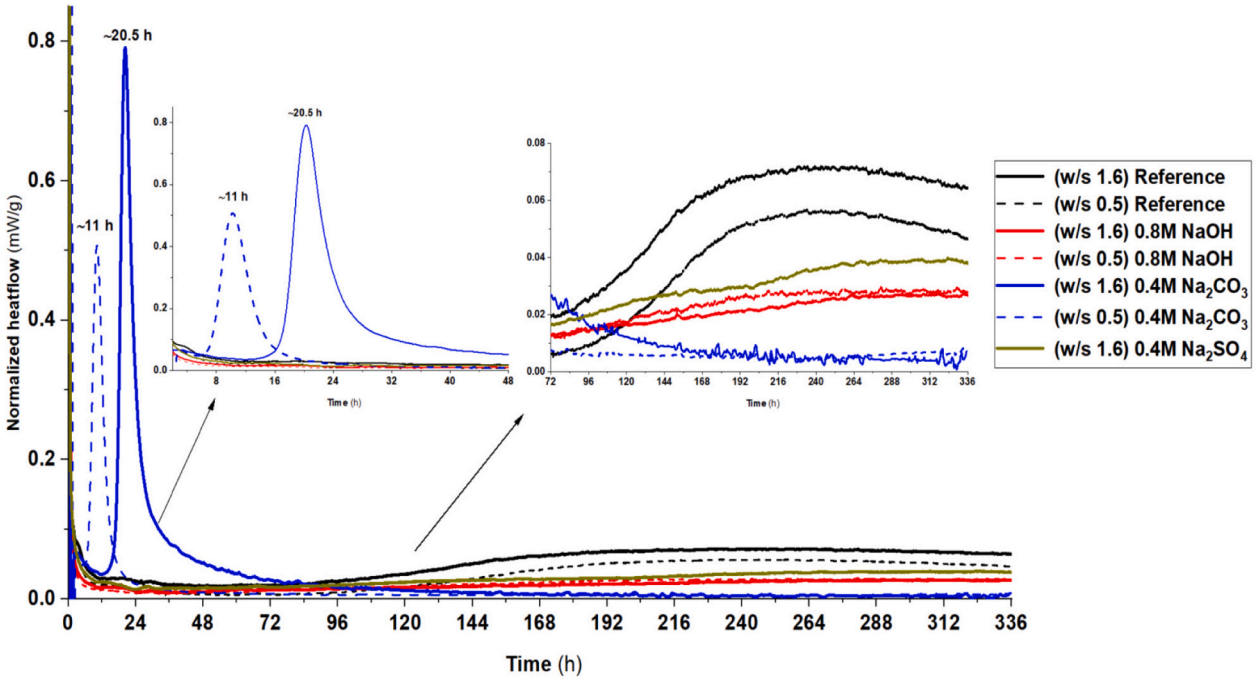

(a)

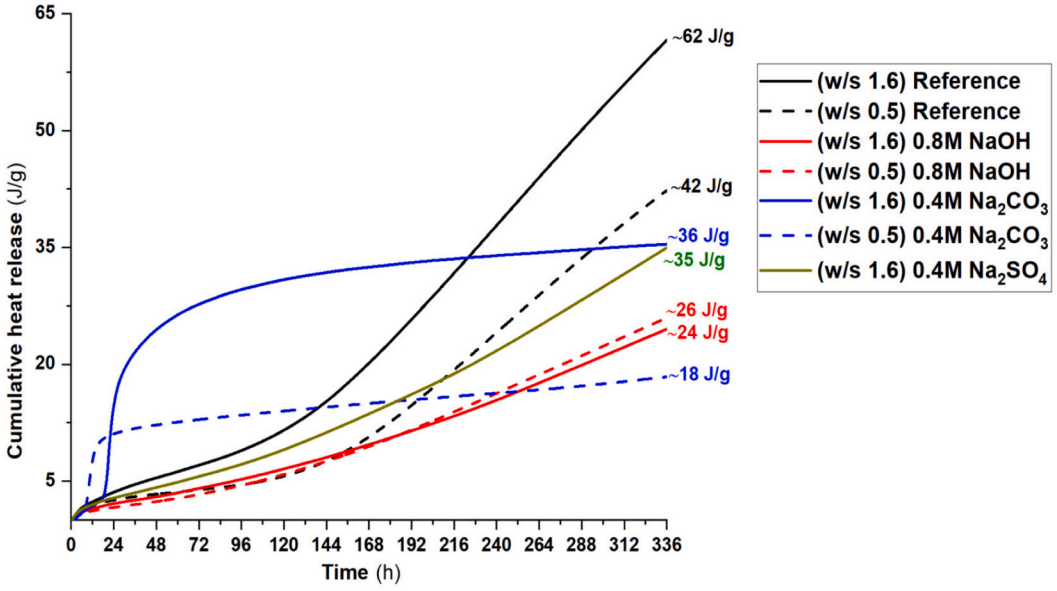

(b)

Fig. 1. Exothermic heat curve of C_2S, hydrated in water-to-solid (w/s) ratio of 1.6 and 0.5 a) normalized heat flow b) cumulative heat of hydration.

sample. After 48 h, no further exothermic heat of hydration was observed in the sodium carbonate sample till 14 days. Decreasing the w/s ratio from 1.6 to 0.5 resulted in shortening the induction period from ~22 to 10 h in the 0.4 M Na_2CO_3 samples indicating that a low dissolution degree is observed to reach equilibrium till 14 days. Moreover, the 0.5 w/s ratio decreases the overall C_2S exothermic heat flow in the reference sample without a significant change in the 0.8 M NaOH sample (Fig. 1 (a)).

The 14 days cumulative heat flow exhibited an increase of 45 and 78%, respectively, upon increasing the 0.5 to 1.6 w/s ratio in the reference as well as the 0.4 M Na_2CO_3 sample. But the overall cumulative heat of hydration is practically the same for sodium hydroxide activator in all w/s ratios (Fig. 1 (b)). These observations indicated that the C_2S dissolution is dependent on the w/s ratio to achieve the solubility equilibrium. The increase in cumulative heat of hydration (~42–62 J/g, ~18–36 J/g) and induction period (~10–22 h) upon increasing the w/s (from 0.5 to 1.6) ratio in reference and 0.4 M Na_2CO_3 sample, respectively, emphasizes the strong dependence of the C_2S dissolution rate on the local ion concentration of OH^- and CO_3^{2-} at the C_2S-grain surface interface [31,32]. Contrary to the previous study [21,33], the 0.4 M Na_2CO_3 sample does not exhibit a higher exothermic heat of hydration than the reference sample. The variations in the results can be attributed to the significant difference ($\Delta E_{activation}$ = ~20–22 kJ/mol) in activation energy with varying β-C_2S surface area [34]. Consequently, the activation energy impacts the hydration process in the rate-controlling step.

At low w/s ratio, the distance from the equilibrium is not high enough and the solution reaches the solubility equilibrium during dissolution [30]. But in the presence of a hydroxide-rich medium such as the 0.8 M NaOH sample, the change in w/s ratio does not impact the cumulative hydration heat (~26 J/g) indicating a very slow dissolution of C_2S. The relatively higher hydroxide concentration close to the surface restricts further silicate dissolution due to strong deprotonation at high pH [35]. The dissolution of C_2S will move in the forward direction only upon precipitation of calcium hydroxide such as:

$$Ca_2SiO_{4\ hydroxylated\ surface} \leftrightarrows 2Ca^{2+} + H_4SiO_4 + 4OH^- \quad (1)$$

$$H_4SiO_4 + OH^- \leftrightarrows H_3SiO_4^- + H_2O \quad (2)$$

$$H_3SiO_4^- + OH^- \leftrightarrows H_2SiO_4^{2-} + H_2O \quad (3)$$

The calorimetric studies indicated that the 1.6 w/s enhances the dissolution degree of C_2S. For this reason, it was adopted for the remaining experiments. Among 0.8 M Na^+ activators in a 1.6 w/s ratio, 0.4 M Na_2CO_3 exhibited higher reactivity within 24 h while showing 41% lower cumulative hydration heat than reference after 14 days of hydration. Moreover, the 0.4 M Na_2SO_4 sample exhibited the same overall cumulative hydration heat (~36 J/g) as the 0.4 M Na_2CO_3 sample at a w/s ratio of 1.6 but showed a steady increase in the heat of hydration after the first 24 h which was not the case for the carbonate sample. As the standard enthalpy of formation (Δ_fH^Θ) suggests a more favorable reaction for calcium sulphate ($CaSO_4$, $\Delta_fH^\Theta = -1434$ kJ/mol) precipitation than calcium carbonate ($CaCO_3$, $\Delta_fH^\Theta = -1208$ kJ/mol) formation [36]. However, the precipitation of the hydration products seems to be controlled by some other factors such as C_2S dissolution-precipitation equilibrium, ionic strength, and pH of the hydration medium [37]. These observations require further insights as provided in the next sections.

3.2. Characterization and order of hydration product formation

As mentioned above, the exothermic heat signals are very low in intensity and different anions particularly SO_4^{2-}, CO_3^{2-}, OH^- etc. can precipitate as calcium sulphate, calcium carbonate, and calcium hydroxide respectively. To understand the events of exothermic hydration reactions, FTIR analysis has been performed on the hydrated sample after 7, 14, and 28 days (see peak assignment Fig. S2 (a, b, c)) as shown in Table 3.

All samples exhibited similar band positions mostly originating from the β-C_2S vibrations. They have narrow band splitting in the range of 800–1200 cm^{-1} corresponding to the Si—O bonds asymmetric and symmetric stretching vibrations of Si—O bands, a band around ~496, 535 cm^{-1} associated to Si—O—Si bending vibrations, and ~450–455 cm^{-1} vibration pointing deformation of SiO_4 tetrahedra. The interaction with air cannot be avoided in the sample, thereby, the bands around 1400–1500 cm^{-1}, and 1640–1650 cm^{-1} are assigned to an asymmetric stretch of CO_3^{2-} and H—O—H bending vibrations of molecular H_2O respectively. The broad band centered around ~3300 cm^{-1} is due to stretching vibrations of hydroxyl groups in H_2O with varying degrees of hydrogen bond strengths [38–40].

After 7 days of curing, the distinct band of C-S-H Q^1 (~815 cm^{-1}) is only observed in the 0.4 M Na_2CO_3 with a distinct carbonate band (~713 cm^{-1}) indicating the precipitation of calcium carbonate as a by-product. But mid-IR bands centered ~3300 cm^{-1} exhibited the strongly ordered hydrogen bonds observed in all the hydrated samples [41]. These bands suggest the presence of C-S-H in all samples, but no distinct band for C-S-H can be assigned. After 14 days of curing, the distinct C-S-H Q^2 (~940–950 cm^{-1}) bands alongside Q^1-type hydration products appear in all the hydrated samples. The relative intensity of the Q^2 (~940–950 cm^{-1}) type bands increased in all the hydrated samples upon 28 days of curing which confirms the polymerization of the silicate chain (Fig. S2 (c)) [16]. Furthermore, the distinct bands ~636, ~616 cm^{-1} and centered around 1100 cm^{-1} indicate the precipitation of gypsum in the 0.4 M Na_2SO_4 sample [42].

Through FTIR analysis, the exothermic reaction observed via calorimetry can be interpreted. At the early stage (0–72 h), the 0.4 M Na_2CO_3 sample exhibited Q^1-type hydration products alongside calcium carbonate. After 3 to 14 days, no exothermic heat event is observed but silicate polymerization occurs, and the Q^2-type hydration product is confirmed. In reference, to 0.8 M NaOH and 0.4 M Na_2SO_4 samples, the

Table 3
General assignments of bands in FTIR fingerprint region.

Band position (cm^{-1})	Assigned to	Signal evolution concerning sample curing age (days)			
		Reference	0.8 M NaOH	0.4 M Na_2CO_3	0.4 M Na_2SO_4
~3643	ν OH [$Ca(OH)_2$]	14, 28	14, 28	14, 28	14, 28
~3360–3315, 2970	ν OH (H_2O)	7, 14, 28	7, 14, 28	7, 14, 28	7, 14, 28
~1640–1650	δ OH (H_2O)	7, 14, 28	7, 14, 28	7, 14, 28	7, 14, 28
~1415–1490	ν_3 CO (CO_3^{2-})	7, 14, 28	7, 14, 28	7, 14, 28	7, 14, 28
~1380–1390, ~1305–1340	δ C—H (aliphatic structure)	14, 28	14, 28	14, 28	14, 28
~1125–1165	ν Si—O	14, 28	14, 28	14, 28	14, 28
~1100–1110	ν_3 SO (SO_4^{2-})	–	–	–	7, 14, 28
~992	ν_3 Si—O—Si (β-C_2S)	7, 14, 28	7, 14, 28	7, 14, 28	7, 14, 28
~940–950	ν Si—O (C-S-H) Q^2	14, 28	14, 28	14, 28	14, 28
~897, 885, 863, 844	ν_3 Si—O—Si (γ/β-C_2S)	7, 14, 28	7, 14, 28	7, 14, 28	7, 14, 28
~815	ν Si—O (C-S-H) Q^1	14, 28	14, 28	7, 14, 28	14, 28
~713	ν_4 CO (CO_3^{2-})	–	–	7, 14, 28	–
~636, 616	ν_4 SO (SO_4^{2-})	–	–	–	7, 14, 28
~537, 495, 436	ν_4 Si—O—Si (γ/β-C_2S)	7, 14, 28	7, 14, 28	7, 14, 28	7, 14, 28
~450–455	δ Si—O (SiO_4 Td)	14, 28	14, 28	7, 14, 28	14, 28

hydration reaction proceeds over time by C-S-H precipitation as well as polymerization as a slow and continuous process as endorsed by calorimetric data. The type of hydration products is further confirmed by the DTG (see Fig. S3 for percentage mass loss). The mass loss events between 50 and 220 °C are attributed to dehydration of C-S-H (also gypsum in case of 0.4 M Na_2SO_4 (Table 3)), 430–510 °C corresponds to dehydration of calcium hydroxide alongside decarbonation of calcium carbonate at 550–800 °C (Fig. 2 (a, b, c)) [43]. All samples hydrated at 7 days exhibited the formation of C-S-H with the highest amount of bound water in 0.4 M Na_2CO_3 sample which confirms the calorimetric results. Upon curing for 14 and 28 days, the C-S-H content was increasing, showing the samples were continuously hydrating except for 0.4 M Na_2CO_3. The reference sample exhibited the highest mass loss associated with C-S-H after 28 days of curing (Fig. 2 (c)).

To understand a correlation between portlandite formation and C-S-H gel-bound water, the $Ca(OH)_2$ as well as $CaCO_3$ wt% amount in the hydrated sample is calculated using the tangential method as expressed in Eq. (4) [29,44]. Moreover, the differences in total bound water were calculated by converting the sample wt% into portlandite and calcite anhydrous mass by Eq. (5). As the sample has undergone carbonation, the carbonate is recalculated to the equivalent amount of portlandite using Eq. (6) under the assumption that the calcite in all samples originates from the carbonation of portlandite. Factor 1.35 refers to the molar mass ratio of $CaCO_3$ (100.09 g/mol) and $Ca(OH)_2$ (74.09 g/mol).

$$m_{measured} = weight\ loss\ (TGA) \times \frac{M_{mineral}}{M_{volatile}} \tag{4}$$

$$m_{anhydrous} = \frac{m_{measured}}{1 - evaporable\ water} \tag{5}$$

$$m_{anhydrous\ Portlandite\ equiv.} = \frac{1.35 \times m_{measured\ calcite} + m_{measured\ Portlandite}}{1 - m_{measured\ calcite} + 1.35 \times m_{measured\ calcite}} \tag{6}$$

weight loss (TGA) = Portlandite (T = ~450–540 °C), Calcite (T = ~550–800 °C),

$M_{mineral}$ = (Portlandite = 74 g/mol), (Calcite = 100 g/mol)

$M_{volatile}$ = (Water = 18 g/mol), (Calcite = 44 g/mol)

evaporable water (wt%) = TGA weight loss (100 − (residual mass + portlandite + calcite))

The comparison between C-S-H gel water and the formation of equivalent anhydrous portlandite amount helped to understand the formation of hydration products as shown in Fig. 3 (a, b). In the reference sample, a clear increase in the C-S-H bound water and portlandite is observed over time. In the 0.8 M NaOH sample, a higher amount of calcium hydroxide (~1.1–4.0 wt%, 7–14 days hydrated sample) was observed as compared to the reference (~0.3–2.1 wt%, 7–14 days hydrated sample) sample while significantly lower (~61%) C-S-H bound water indicates the lower reactivity of C_2S contrary to previous study [13]. These results indicate the earlier precipitation of portlandite in 0.8 M NaOH sample compared to the reference would lead to the slow dissolution of C_2S. A serious decrease in the dissolution of C_2S is

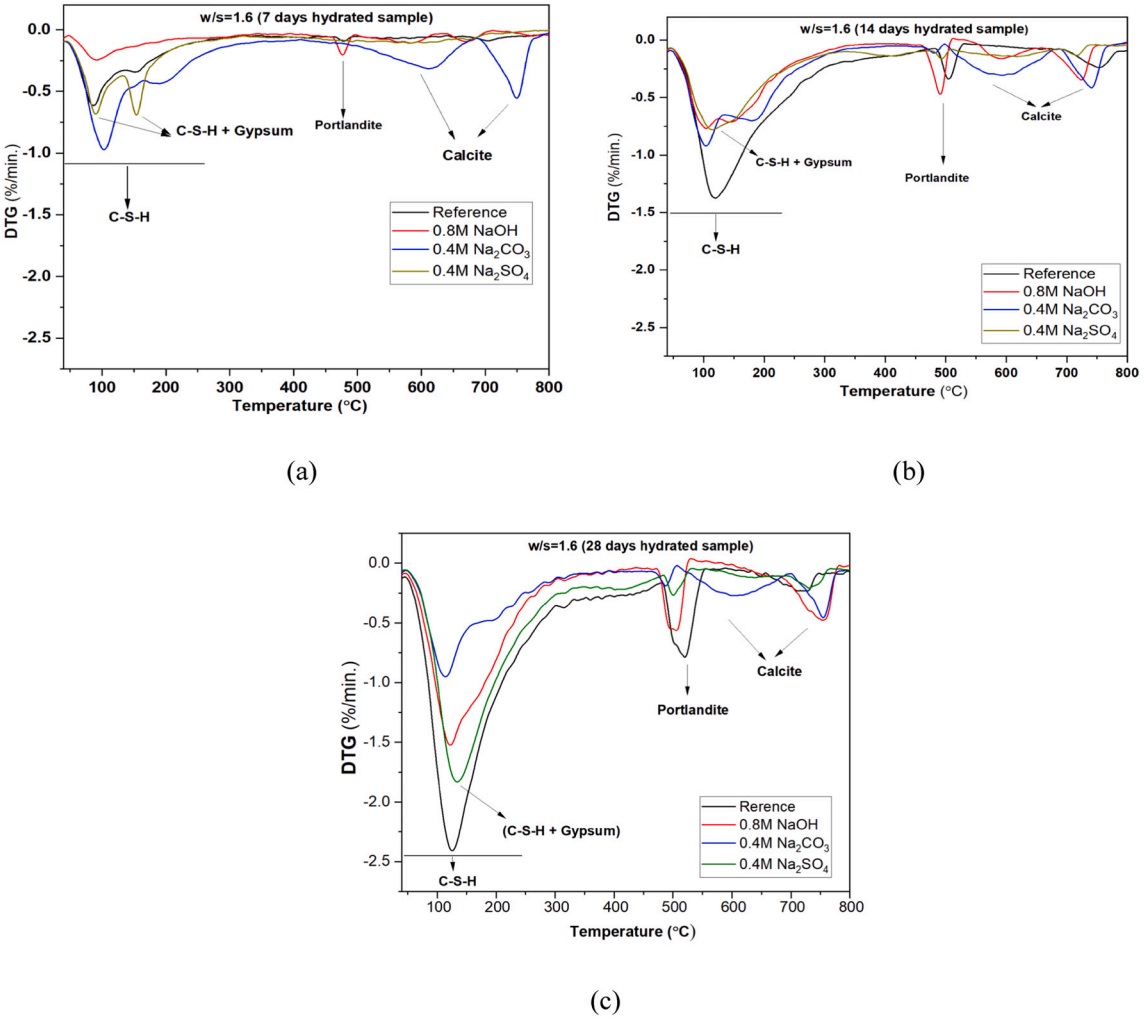

Fig. 2. Differential thermal gravimetric (DTG) analysis of chemically activated C_2S at curing age of a) 7 b) 14 and c) 28 days with 1.6 w/s ratio.

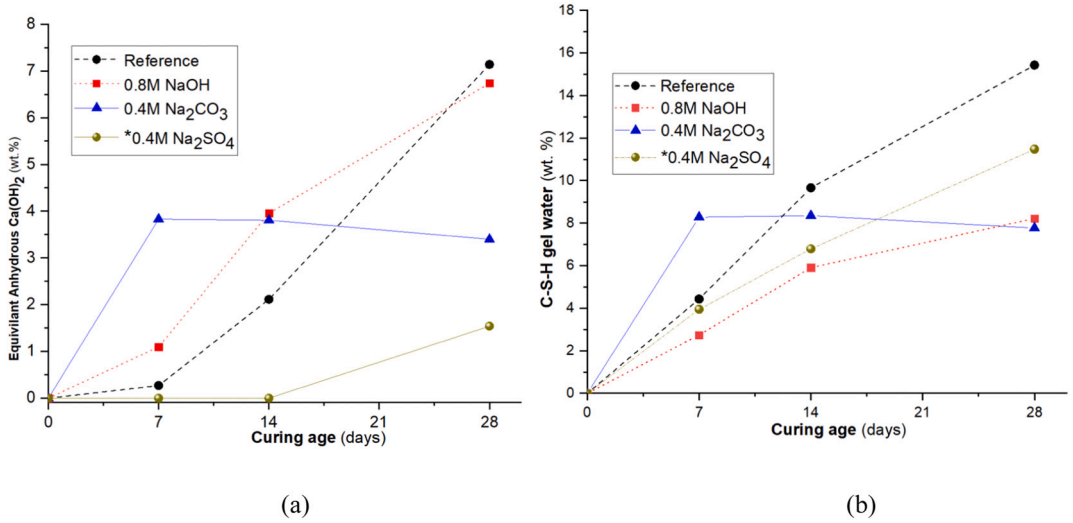

Fig. 3. Calculation of chemically bound water over time of chemically activated C_2S a) equivalent anhydrous portlandite (wt%) via Eq. (6). b) calcium silicate hydrate (C-S-H) gel water (wt%) or evaporable water (Eq. (5)). *It is not possible to differentiate between weight loss event of gypsum and C-S-H in 0.4 M Na_2SO_4 sample (Fig. 2). Because the C-S-H volatiles coincides with the gypsum water of crystallization.

reported in the presence of a high initial concentration of portlandite [45]. However, if a very high supersaturation with respect to portlandite could be maintained, the portlandite and C-S-H nucleation can happen without the need for high dissolution [46]. That is usually observed at high concentrations of NaOH/KOH activated C_2S reaction [13] but low concentration delays the hydration as observed in 0.8 M NaOH sample. Furthermore, the hydroxyl ions-rich solution promotes the precipitation of calcium hydroxide leading to a possible decrease in the Ca/Si ratio due to less calcium available for incorporation in C-S-H as the solubility of calcium hydroxide decreases at high pH.

In the 0.4 M Na_2CO_3 sample, the amount of equiv. calcium hydroxide and C-S-H bound water remain constant once they are precipitated. After 14 days, a slightly lower mass loss for the gel water can be attributed to the enriching of C-S-H with Q^2-type silicate chains (Table 3). In the 0.4 M Na_2SO_4 sample, the calculation of C-S-H volatiles was difficult because the gel water weight loss overlaps with the bound water of gypsum (~100–200 °C). So, the C-S-H gel amount is high because it also contains gypsum water for crystallization.

C_2S hydration reaction products are confirmed via QXRD as shown in Fig. 4 (see Fig. S2 (b, c, d) for new hydration product peak assignment of the hydrated sample) and normalize to the portlandite ($m_{measured}$) mass from TG analysis. The presence of β-C_2S hydration by-products such as portlandite, calcite, and gypsum are observed for 28 days. In the 0.4 M Na_2SO_4 sample, gypsum is observed only in 7 days hydrated sample while at a later stage (14 and 28 days), only portlandite is visible. The pH of the 0.4 M Na_2SO_4 sample was found to be in the range of 12.5–13.0 measured at random moments between 5 and 12 days. The dissolution of gypsum increases at pH 12–13 [47] explaining why, no gypsum crystal is observed at later stages (14 and 28 days cured samples).

The degree of hydration (DOH) is calculated by using: As the hydrated β-C_2S mass partially consists of bound water and is corrected from the TGA mass loss.

$$DOH\ (\%)\ t_x = \frac{mXRD_{\beta C2S}t_0 - mXRD_{\beta C2S}t_x(1 - evaporable\ water)}{mXRD_{\beta C2S}t_0} \quad (7)$$

At 7 days of hydration, the DOH was 60% higher for 0.4 M Na_2CO_3 than the reference sample. So, only the carbonate accelerates the hydrationat an early age. In the 0.4 M Na_2SO_4 sample, the highest DOH

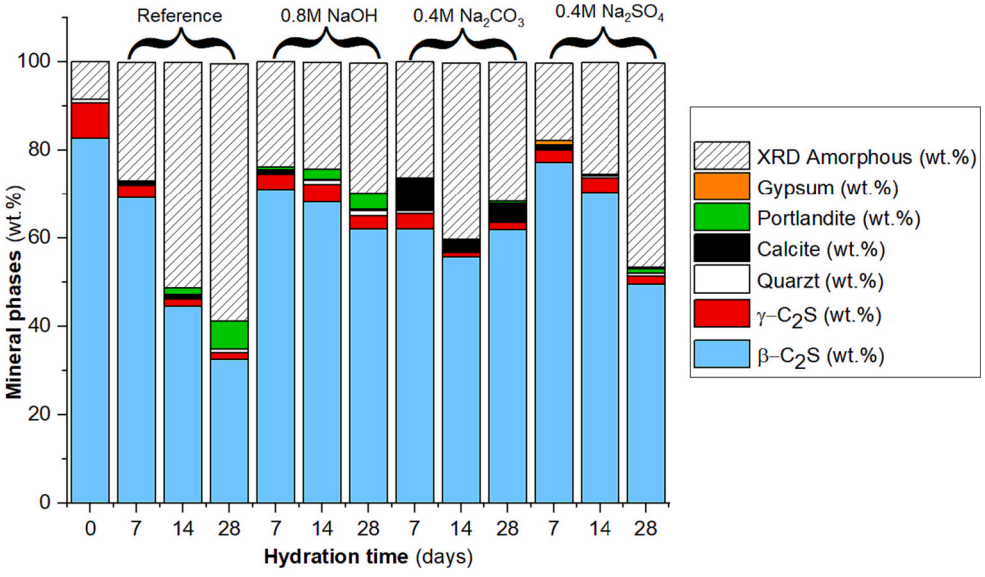

Fig. 4. Quantitative X-ray diffraction (QXRD) of chemically activated β-C_2S at curing ages of 7, 14, and 28 days with a 1.6 w/s ratio.

(~223%) increase was observed at curing age between 14 and 28 days. The increase in hydration can be attributed to the dissolution of calcium sulphate at high pH (12-13) and promotes C-S-H precipitation leading to an increase in C_2S dissolution [47]. As NaOH is described as an alkali activator but the present result argues that hydration in 0.8 M NaOH lowers the β-C_2S reactivity at every age [25]. Overall, the reference sample exhibited a continuous increase and reaches 67% until 28 days as shown in Fig. 5. At 28 days of hydration, the addition of various anions lowered the degree of hydration. For 0.8 M NaOH, 0.4 M Na_2CO_3, and 0.4 M Na_2SO_4 samples, a decrease of ~54%, ~54%, and ~30%, respectively, in hydration degree was measured.

The morphology of the hydration product in the presence of varying anions has been presented in Fig. 6. The reference sample exhibited a densely interconnected structure in the early stage (7 days) which changes into well distributed wider needle-like structure in the later stage of curing (Fig. 6 (a, b)) [46]. In the case of carbonate anion-rich hydration medium, the C-S-H structure exhibited the crumbled foil structure alongside rhombohedral agglomerated calcite crystal (Fig. 6 (c, d)). For the 0.8 M NaOH sample, a fibrous morphology of the C-S-H was observed alongside the hexagonal crystal of portlandite (Fig. 6 (e)). A dense aggregated network with possible gypsum crystal was observed in the sulphate-activated sample (Fig. 6 (f)). The varying morphology of C-S-H is dependent on the Ca/Si ratio and type of activator [18,26,48].

By comparing all the anion's behaviour in C_2S activation, it is observed that the 0.4 M Na_2CO_3 sample exhibited high hydration activity at an early stage (7 days) and undergoes an apparent dormant period that lasts for at least 28 days. On the contrary, a slow and continuous β-C_2S hydration process is observed in the reference sample which attains a high reaction degree at a later stage (14–28 days). In the presence of sulphate anions, pH seems to play an important role in the dissolution-precipitation of gypsum, calcite, and portlandite respectively. Moreover, the hydroxyl-rich medium caused the early precipitation of portlandite which significantly decreases the β-C_2S hydration reaction over time. To understand the different β-C_2S hydration behaviour in water and sodium carbonate at an early stage, *in-situ* pH and conductivity are measured during hydration. The conductivity of the solution is a measure of ions concentration and mobility in a solution at a given temperature. As the concentration of hydroxyl ions and the ionic strength of hydration mediums play an important role in the C_2S reactivity.

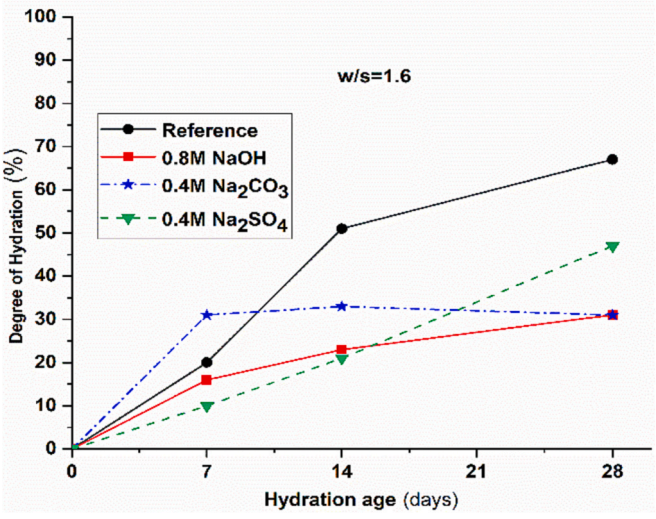

Fig. 5. Degree of hydration (DOH) of chemically activated β-C_2S calculated via QXRD and TGA over 28 days.

3.3. *In-situ pH and conductivity measurement*

The evolution of hydroxyl ion concentration and ionic conductivity was measured for the reference and 0.4 M Na_2CO_3 samples during the first 5 days as shown in Fig. 7. It is worth mentioning here that the same temperature condition such as 20 ± 2 °C as well as a 1.6 water to solid ratio was chosen to have comparable results with calorimetric data. In the reference sample, a continuous increase in pH and conductivity is observed till ~60 h indicating the continuous dissolution of C_2S. After 60 h, the pH attains a plateau, but the conductivity still increases which can be attributed to the high activity event of precipitation of the hydration product (Fig. 7 (a)). In the case of the 0.4 M Na_2CO_3 sample, a clear increase in the hydroxyl ion concentration and conductivity was observed around ~15 h which can be dominantly attributed to the β-C_2S dissolution. After ~15 h an acceleration period of precipitation-dissolution last for a further ~6 h followed by a clear decrease in the ionic concentration in the solution. However, the concentration of hydroxyl ions remains high (pH ≅ 13.1), and ionic mobility around ~40 h attains its plateau indicating the solution attaining the equilibrium (Fig. 7 (b)). So, the proposed chemical reaction can be written as follow:

$$Ca_2SiO_{4\ (s)} + 2H_2O \leftrightarrow 2Ca^{2+} + 4OH^- + H_4SiO_4 \quad (8)$$

$$Ca(OH)_{2\ (aq)} + CO^{2-}_{3\ (aq)} \rightarrow CaCO_{3\ (s)} + 2OH^-_{(aq)} \quad (9)$$

A basic dissolution medium does not enhance the dissolution of dicalcium silicate. A high pH (~13) leads to a negative surface charge that further limits the solubility (Eqs. (2), (3)). The high negative surface charge attracts the Ca^{2+} or Na^+ ions strongly. Moreover, the precipitation of $CaCO_3$ increases at high pH. The simultaneous precipitation of C-S-H and calcium carbonate deprives the solution of transportable cations between the solid surface and the solution leading to a longer dynamic equilibrium state for 0.4 M Na_2CO_3 from 2 to 28 days at high pH (~13.0). The term dynamic equilibrium rather than steady-state equilibrium is used because no net change in the hydration degree till 28 days was observed. Moreover, the simultaneous precipitation of calcium carbonate leads to fewer calcium ions available to get incorporated in C-S-H.

If the lack of transportable cations in the 0.4 M Na_2CO_3 sample is the leading cause for the longer equilibrium at high pH, then any solid surface site that has a high affinity for the Ca^{2+} would speed up the dissolution-precipitation reaction. To test the hypothesis, the 3 wt% $CaCO_3$ is provided as a nucleation site for the Ca^{2+} ions.

3.4. *Effect of $CaCO_3$ as a nucleation site for Ca^{2+} ions*

The exothermic heat of the reaction of various samples with 3 wt% added $CaCO_3$ has been presented in Fig. 8. In the 0.4 M Na_2CO_3 sample, the presence of solid calcium carbonate shortens the induction period from ~15 to 3 h. Consequently, the time for the heat of hydration peak maxima reduces from ~22 to 11 h and the system early reaches into dynamic equilibrium state (Fig. 8 (a)). But overall, the addition of calcium carbonate did not lead to any change in the cumulative heat release (~36 J/g) (Fig. 8 (b)). These findings indicate that the lack of transportable cations between a solid surface and solution leads to a dormant period from 2 to 28 days making β-C_2S dissolution highly discontinuous as compared to a reference, 0.4 M Na_2SO_4 and 0.8 M NaOH samples. In the case of the reference and 0.8 M NaOH sample, the provision of calcium carbonate as an inert material seriously slows the hydration reaction compared to the reaction without added calcite (Fig. 1). The presence of $CaCO_3$ does not have this effect in the Na_2CO_3 sample.

Overall, the C_2S reactivity in the presence of anions such as CO_3^{2-}, SO_4^{2-} and OH^- etc. can be broadly divided into three different cases: C_2S dissolution-precipitation reaction (case I), simultaneous precipitation of C-S-H and carbonates (case II): An early precipitation of reaction byproducts such as portlandite, gypsum, etc. (case III).

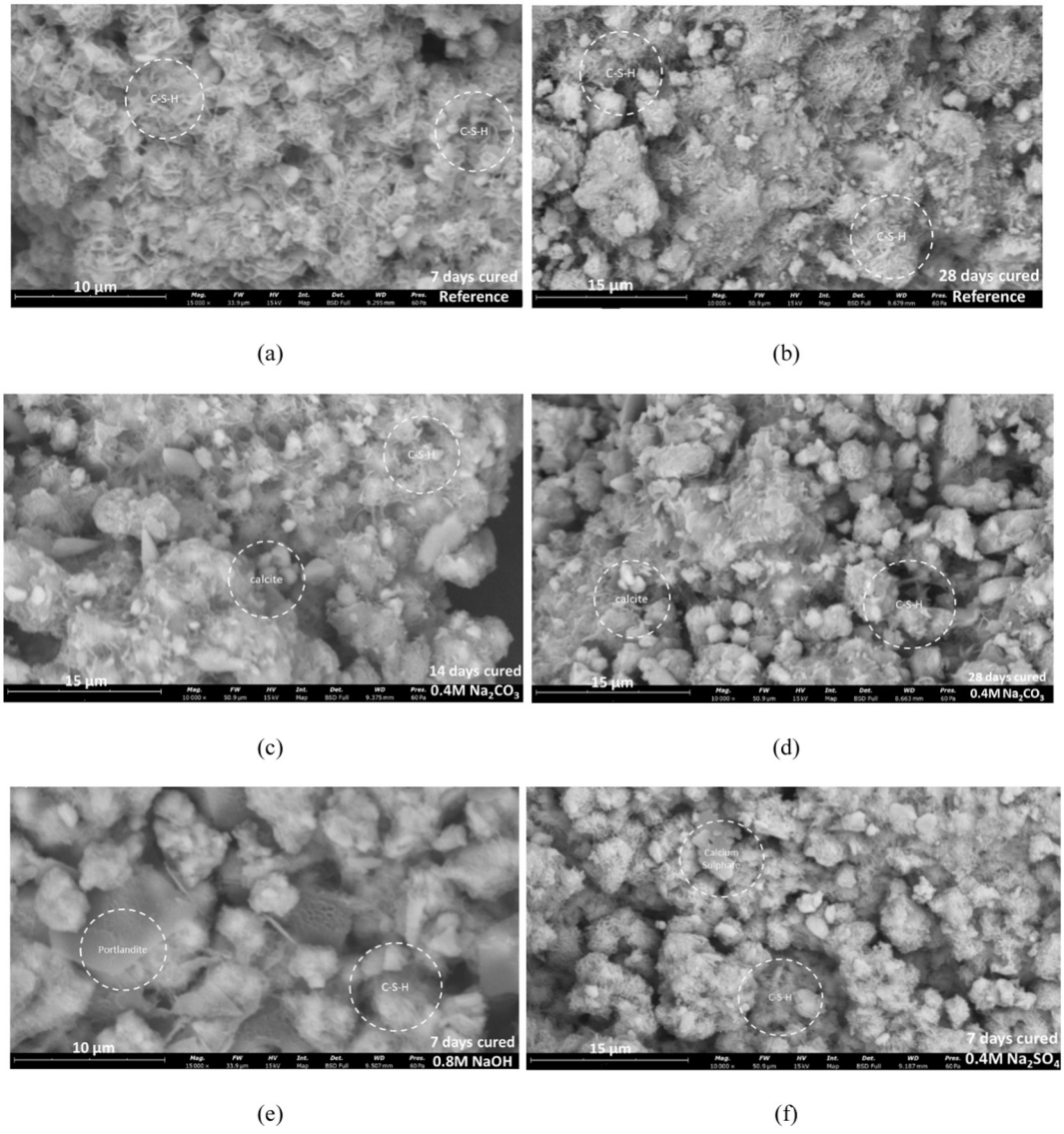

Fig. 6. Scanning electron microscopy (SEM) micrographs of chemically activated β-C_2S a) 7 days cured b) 28 days cured reference sample c) 14 days cured d) 28 days cured 0.4 M Na_2CO_3 e) 7 days cured 0.8 M NaOH and f) 0.4 M Na_2SO_4 samples.

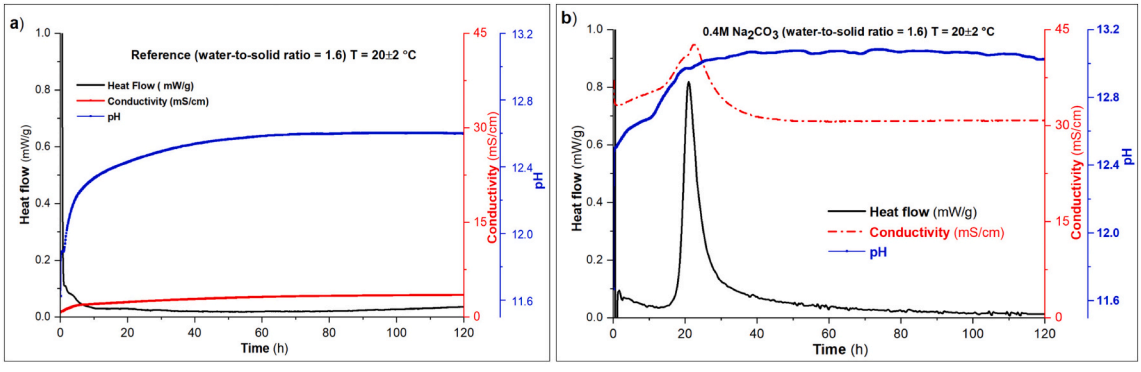

Fig. 7. In situ pH, conductivity, and isothermal calorimetric analysis at 20 °C of a) reference b) 0.4 M Na_2CO_3 sample.

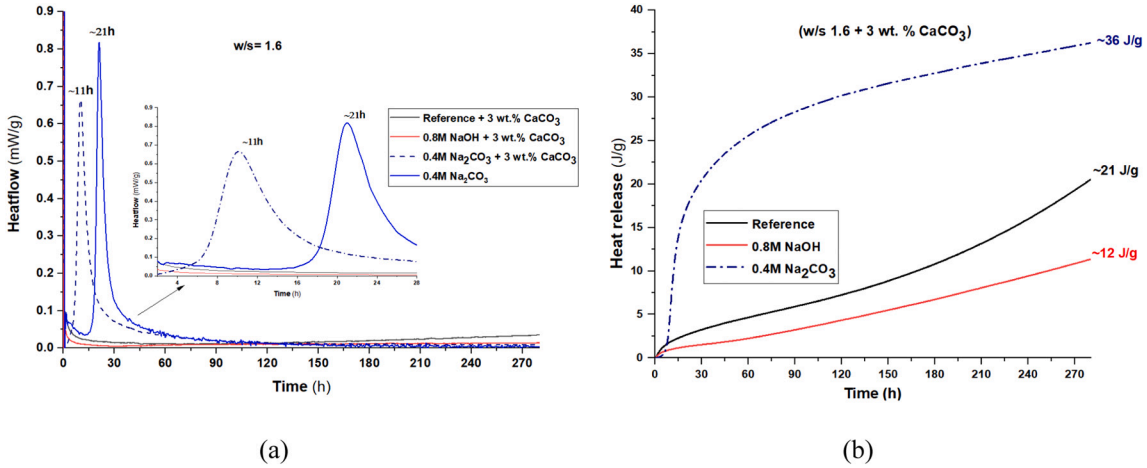

Fig. 8. Exothermic heat curve of chemically activated β-C_2S in the presence of 3 wt% $CaCO_3$ a) normalized heat flow b) cumulative heat of hydration.

Case I: The standard C_2S reaction in the reference sample exhibited a dissolution equilibrium followed by precipitation of C-S-H. The important point to mention here is that the C-S-H precipitates earlier than the portlandite. That is why, the least amount of equivalent anhydrous portlandite (~0.3 wt%) is observed after 7 days of hydration. Moreover, the changes in the w/s ratio markedly shift the dissolution equilibrium which emphasizes the importance of local ion concentration at the C_2S-grain surface interface that predominantly plays an important role in C_2S reactivity [31,45].

Case II: In the case of 0.4 M Na_2CO_3, simultaneous precipitation of C-S-H and calcite leaves the solution enriched with hydroxyl ions. Due to the high hydroxyl ion concentration in the solution, the silicate surface got deprotonated and become negatively charged. The negatively charged surface not only restricts the C_2S dissolution but also hinders the diffusion of cations between the solid surface and the solution in this case.

Case III: In the case of 0.8 M NaOH, early precipitation of portlandite (Equiv. anhydrous portlandite (~1.1 wt%) 366 times more than the reference (0.3 wt%) sample) seriously delays the C-S-H precipitation. The same is observed for the 0.4 M Na_2SO_4 sample at an early stage (7 days). But the calcium sulphate (gypsum) is more soluble at high pH than portlandite. So, the dissolution over time saturates the solution to promote C-S-H precipitation. Therefore, the highest DOH (~223%) increase was observed in the 0.4 M Na_2SO_4 sample between the age of 14 and 28 days.

4. Conclusion

The effect of fixed moles of (0.8 M) Na^+ cations balanced by either OH^-, SO_4^{2-} or CO_3^{2-} anions on β-C_2S hydration was investigated at ambient temperature. The important findings are as follows.

β-C_2S reactivity is highly dependent on the water-to-solid ratio. The increase in w/s ratio from 0.5 to 1.6 significantly increases C_2S dissolution leading to a 47 and 100% increase in cumulative hydration heat (14 days) respectively, in reference as well as 0.4 M Na_2CO_3. But in 0.8 M NaOH, the change in w/s ratio did not alter the cumulative hydration degree indicating the slowing of C_2S dissolution.

β-C_2S hydration reaction proceeds over time by dissolution equilibrium, C-S-H/portlandite precipitation, and silicate chain polymerization as a slow and continuous process. The β-C_2S reactivity exhibited a continuous increase in hydration degree (DOH) and reaches the highest 67% at 28 days hydrated reference sample.

At 7 days, the carbonate-activated β-C_2S exhibited a 55% higher DOH than the reference. But at later ages (7–28 days), no further hydration activity was observed except for the polymerization of silicate chains (enrichment with Q^2 (C-S-H) type units). The apparent dormant period is attributed to the simultaneous precipitation of C-S-H and calcium carbonate depriving the solution of transportable cations between the solid surface and hydration medium at high pH (~13.1). The idea is further confirmed by the addition of 3 wt% calcium carbonate as nucleation site that further reduced the induction period from ~22 to 11 h without changing the overall cumulative heat of hydration.

The β-C_2S hydration of sulphate-rich ions is more dependent on the pH. At first, gypsum was found to be the only hydration product alongside C-S-H at 7 days. As the C_2S dissolution increases so does the pH of the hydration medium, the gypsum started to dissolve and portlandite precipitates at later stages. At curing age between 14 and 28 days, the highest DOH (~223%) was observed which is attributed to the calcium sulphate dissolution, and the promotion of C-S-H precipitation.

0.8 M NaOH activated β-C_2S exhibited no significant increase in hydration degree at any stage compared to the reference sample leading to the lowest DOH (~31%) after 28 days. This behaviour is attributed to the early precipitation of portlandite and the high pH of the solution leading to the slow dissolution of β-C_2S.

CRediT authorship contribution statement

Muhammad Jawad Ahmed: Conceptualization, Methodology, Validation, Investigation, Writing – original draft, Writing – review & editing. **Kim Lambrechts:** Conceptualization, Methodology, Investigation, Validation. **Xuan Ling:** Methodology, Investigation. **Katrin Schollbach:** Resources, Visualization, Writing – review & editing, Supervision. **H.J.H. Brouwers:** Resources, Visualization, Writing – review & editing, Project administration, Supervision.

Declaration of competing interest

The authors declare that they have no known competing financial interests or personal relationships that could have appeared to influence the work reported in this paper.

Data availability

Data will be made available on request.

Acknowledgment

The authors would like to acknowledge the financial support by NWO (The Netherlands Organisation for Scientific Research) for funding this research (project no. 10023338) and M2i (Materials Innovation Institute, project no. S81.6.15565b) for managing this project. Additionally, the authors wish to express their appreciation to Sieger van der

Laan for his revision and guidance. Furthermore, the authors wish to express their gratitude to the following sponsors of this research: Tata Steel; ENCI; V.d. Bosch Beton; Blue Phoenix Group; Hess.

Appendix A. Supplementary data

Supplementary data to this article can be found online at https://doi.org/10.1016/j.cemconres.2023.107302.

References

[1] A.K. Chatterjee, High belite cements—present status and future technological options: part I, Cem. Concr. Res. 26 (1996) 1213–1225, https://doi.org/10.1016/0008-8846(96)00099-3.
[2] A. Cuesta, A. Ayuela, M.A.G. Aranda, Belite cements and their activation, Cem. Concr. Res. 140 (2021), 106319, https://doi.org/10.1016/j.cemconres.2020.106319.
[3] W.F. Santos, K. Schollbach, S. Melzer, S.R. van der Laan, H.J.H. Brouwers, Quantitative analysis and phase assemblage of basic oxygen furnace slag hydration, J. Hazard. Mater. 450 (2023), https://doi.org/10.1016/J.JHAZMAT.2023.131029.
[4] E. Gartner, H. Hirao, A review of alternative approaches to the reduction of CO_2 emissions associated with the manufacture of the binder phase in concrete, Cem. Concr. Res. 78 (2015) 126–142, https://doi.org/10.1016/J.CEMCONRES.2015.04.012.
[5] M. Ben Haha, F. Winnefeld, A. Pisch, Advances in understanding ye'elimite-rich cements, Cem. Concr. Res. 123 (2019), 105778, https://doi.org/10.1016/J.CEMCONRES.2019.105778.
[6] T. Staněk, P. Sulovský, Active low-energy belite cement, Cem. Concr. Res. (2015), https://doi.org/10.1016/j.cemconres.2014.11.004.
[7] N. Elfami, H. Ez-zaki, A. Diouri, O. Sassi, A. Boukhari, Improvement of hydraulic and mechanical properties of dicalcium silicate by alkaline activation, Constr. Build. Mater. 247 (2020), 118589, https://doi.org/10.1016/J.CONBUILDMAT.2020.118589.
[8] A.J.M. Cuberos, Á.G. De la Torre, M.C. Martín-Sedeño, L. Moreno-Real, M. Merlini, L.M. Ordónez, M.A.G. Aranda, Phase development in conventional and active belite cement pastes by Rietveld analysis and chemical constraints, Cem. Concr. Res. 39 (2009) 833–842, https://doi.org/10.1016/J.CEMCONRES.2009.06.017.
[9] A. Bouregba, H. Ez-zaki, A. Diouri, O. Sassi, Dicalcium silicate hydration behavior in the presence of Na_2CO_3 and water glass, Asian J. Civ. Eng. 20 (2019) 857–867, https://doi.org/10.1007/s42107-019-00150-0.
[10] A. Cuesta, E.R. Losilla, M.A.G. Aranda, J. Sanz, Á.G. De La Torre, Reactive belite stabilization mechanisms by boron-bearing dopants, Cem. Concr. Res. 42 (2012) 598–606, https://doi.org/10.1016/j.cemconres.2012.01.006.
[11] T. Stanek, P. Sulovský, D. Vsianský, Active belite clinker doped with SO_3, in: 13th Int. Congr. Chem. Cem, 2011, pp. 1–7.
[12] H. El-Didamony, A.M. Sharara, I.M. Helmy, S. Abd El-Aleem, Hydration characteristics of β-C2S in the presence of some accelerators, Cem. Concr. Res. 26 (1996) 1179–1187, https://doi.org/10.1016/0008-8846(96)00103-2.
[13] M.J. Sánchez-Herrero, A. Fern Andez-Jim Enez, A. Palomo, Alkaline hydration of C2S and C3S, J. Am. Ceram. Soc. 99 (2015), https://doi.org/10.1111/jace.13985.
[14] I. García Lodeiro, A. Fernández-Jimenez, A. Palomo, D.E. Macphee, Effect on fresh C-S-H gels of the simultaneous addition of alkali and aluminium, Cem. Concr. Res. 40 (2010) 27–32, https://doi.org/10.1016/J.CEMCONRES.2009.08.004.
[15] T. Kim, M.F. Alnahhal, Q.D. Nguyen, P. Panchmatia, A. Hajimohammadi, A. Castel, Initial sequence for alkali-silica reaction: transport barrier and spatial distribution of reaction products, Cem. Concr. Compos. 104 (2019), 103378, https://doi.org/10.1016/J.CEMCONCOMP.2019.103378.
[16] Y. Yan, S.Y. Yang, G.D. Miron, I.E. Collings, E. L'Hôpital, J. Skibsted, F. Winnefeld, K. Scrivener, B. Lothenbach, Effect of alkali hydroxide on calcium silicate hydrate (C-S-H), Cem. Concr. Res. 151 (2022), 106636, https://doi.org/10.1016/J.CEMCONRES.2021.106636.
[17] N. Elfami, H. Ez-zaki, A. Diouri, O. Sassi, A. Boukhari, Improvement of hydraulic and mechanical properties of dicalcium silicate by alkaline activation, Constr. Build. Mater. 247 (2020), https://doi.org/10.1016/j.conbuildmat.2020.118589.
[18] C.K. Park, Effects of alkalies on hydration of β-dicalcium silicate and its resultant hydrates, J. Ceram. Soc. Japan 108 (2000) 113–117, https://doi.org/10.2109/jcersj.108.1254_113.
[19] L. Nicoleau, M.A. Bertolim, Analytical model for the alite (C3S) dissolution topography, J. Am. Ceram. Soc. 99 (2016) 773–786, https://doi.org/10.1111/JACE.13647.
[20] I. García Lodeiro, D.E. Macphee, A. Palomo, A. Fernández-Jiménez, Effect of alkalis on fresh C-S-H gels. FTIR analysis, Cem. Concr. Res. 39 (2009) 147–153, https://doi.org/10.1016/j.cemconres.2009.01.003.
[21] M.J. Sánchez-Herrero, A. Fernández-Jiménez, A. Palomo, C3S and C2S hydration in the presence of Na_2CO_3 and Na_2SO_4, J. Am. Ceram. Soc. 100 (2017) 3188–3198, https://doi.org/10.1111/jace.14855.
[22] W. Kunther, S. Ferreiro, J. Skibsted, Influence of the Ca/Si ratio on the compressive strength of cementitious calcium–silicate–hydrate binders, J. Mater. Chem. A 5 (2017) 17401–17412, https://doi.org/10.1039/C7TA06104H.
[23] I.G. Richardson, Nature of C-S-H in hardened cements, Cem. Concr. Res. 29 (1999) 1131–1147, https://doi.org/10.1016/S0008-8846(99)00168-4.
[24] M.M. Radwan, H.K. Abd El-Hamid, A.F. Mohamed, Influence of saline solution on hydration behavior of β-dicalcium silicate in comparison with biphasic calcium phosphate/hydroxyapatite bio-ceramics, Mater. Sci. Eng. C 57 (2015) 355–362, https://doi.org/10.1016/j.msec.2015.07.011.
[25] H. El-Didamony, A.M. Sharara, I.M. Helmy, S. Abd El-Aleem, Hydration characteristics of β-C2S in the presence of some accelerators, Cem. Concr. Res. 26 (1996) 1179–1187, https://doi.org/10.1016/0008-8846(96)00103-2.
[26] J. Zhang, W. Zhang, J. Ye, X. Ren, L. Liu, W. Shen, Influence of alkaline carbonates on the hydration characteristics of β-C2S, Constr. Build. Mater. 296 (2021), 123661, https://doi.org/10.1016/J.CONBUILDMAT.2021.123661.
[27] K. Scrivener, A. Ouzia, P. Juilland, A. Kunhi Mohamed, Advances in understanding cement hydration mechanisms, Cem. Concr. Res. 124 (2019), 105823, https://doi.org/10.1016/J.CEMCONRES.2019.105823.
[28] M. Jawad Ahmed, K. Schollbach, S. van der Laan, M. Florea, H.J. Brouwers, A quantitative analysis of dicalcium silicate synthesized via different sol-gel methods, Mater. Des. 213 (2022), 110329, https://doi.org/10.1016/j.matdes.2021.110329.
[29] K. Scrivener, R. Snellings, B. Lothenbach, A Practical Guide to Microstructural Analysis of Cementitious Materials, CRC Press, Boca Raton, 2016.
[30] E. Durgun, H. Manzano, R.J.M. Pellenq, J.C. Grossman, Understanding and controlling the reactivity of the calcium silicate phases from first principles, Chem. Mater. (2012), https://doi.org/10.1021/cm203127m.
[31] A.S. Brand, J.M. Gorham, J.W. Bullard, Dissolution rate spectra of β-dicalcium silicate in water of varying activity, Cem. Concr. Res. 118 (2019) 69–83, https://doi.org/10.1016/J.CEMCONRES.2019.02.014.
[32] K.L. Scrivener, P. Juilland, P.J.M. Monteiro, Advances in understanding hydration of Portland cement, Cem. Concr. Res. 78 (2015) 38–56, https://doi.org/10.1016/j.cemconres.2015.05.025.
[33] J. Zhang, W. Zhang, J. Ye, X. Ren, L. Liu, W. Shen, Influence of alkaline carbonates on the hydration characteristics of β-C2S, Constr. Build. Mater. 296 (2021), 123661, https://doi.org/10.1016/j.conbuildmat.2021.123661.
[34] J.J. Thomas, S. Ghazizadeh, E. Masoero, Kinetic mechanisms and activation energies for hydration of standard and highly reactive forms of β-dicalcium silicate (C2S), Cem. Concr. Res. 100 (2017) 322–328, https://doi.org/10.1016/j.cemconres.2017.06.001.
[35] E. Bernard, Y. Yan, B. Lothenbach, Effective cation exchange capacity of calcium silicate hydrates (C-S-H), Cem. Concr. Res. 143 (2021), 106393, https://doi.org/10.1016/j.cemconres.2021.106393.
[36] J.R. Rumble, CRC Handbook of Chemistry and Physics, 102nd ed., CRC Press/Taylor & Francis Group, Boca Raton, 2021.
[37] D.I. Stewart, A.W. Bray, G. Udoma, A.J. Hobson, W.M. Mayes, M. Rogerson, I. T. Burke, Hydration of dicalcium silicate and diffusion through neo-formed calcium-silicate-hydrates at weathered surfaces control the long-term leaching behaviour of basic oxygen furnace (BOF) steelmaking slag, Environ. Sci. Pollut. Res. 25 (2018) 9861–9872, https://doi.org/10.1007/S11356-018-1260-7/FIGURES/5.
[38] N.Y. Mostafa, E.A. Kishar, S.A. Abo-El-Enein, FTIR study and cation exchange capacity of Fe^{3+}- and Mg^{2+}-substituted calcium silicate hydrates, J. Alloys Compd. 473 (2009) 538–542, https://doi.org/10.1016/J.JALLCOM.2008.06.029.
[39] E. John, D. Stephan, Calcium silicate hydrate—in-situ development of the silicate structure followed by infrared spectroscopy, J. Am. Ceram. Soc. 104 (2021) 6611–6624, https://doi.org/10.1111/JACE.18019.
[40] Y. Ping, R.J. Kirkpatrick, P. Brent, P.F. McMillan, X. Cong, Structure of calcium silicate hydrate (C-S-H): near-, mid-, and far-infrared spectroscopy, J. Am. Ceram. Soc. 82 (1999) 742–748, https://doi.org/10.1111/J.1151-2916.1999.TB01826.X.
[41] F.B. Reig, J.V.G. Adelantado, M.C.M. Moya Moreno, FTIR quantitative analysis of calcium carbonate (calcite) and silica (quartz) mixtures using the constant ratio method. Application to geological samples, Talanta 58 (2002) 811–821, https://doi.org/10.1016/S0039-9140(02)00372-7.
[42] P.S.R. Prasad, V.K. Chaitanya, K.S. Prasad, D.N. Rao, Direct formation of the γ-$CaSO_4$ phase in dehydration process of gypsum: in situ FTIR study, Am. Mineral. 90 (2005) 672–678, https://doi.org/10.2138/AM.2005.1742/MACHINEREADABLECITATION/RIS.
[43] M. Jawad Ahmed, W. Franco Santos, H.J.H. Brouwers, Air granulated basic oxygen furnace (BOF) slag application as a binder: effect on strength, volumetric stability, hydration study, and environmental risk, Constr. Build. Mater. 367 (2023), 130342, https://doi.org/10.1016/J.CONBUILDMAT.2023.130342.
[44] Y.A. Villagrán-Zaccardi, H. Egüez-Alava, K. De Buysser, E. Gruyaert, N. De Belie, Calibrated quantitative thermogravimetric analysis for the determination of portlandite and calcite content in hydrated cementitious systems, Mater. Struct. Constr. 50 (2017) 1–10, https://doi.org/10.1617/S11527-017-1046-2/TABLES/3.
[45] L. Nicoleau, A. Nonat, D. Perrey, The di- and tricalcium silicate dissolutions, Cem. Concr. Res. (2013), https://doi.org/10.1016/j.cemconres.2013.01.017.
[46] J.W. Bullard, H.M. Jennings, R.A. Livingston, A. Nonat, G.W. Scherer, J. S. Schweitzer, K.L. Scrivener, J.J. Thomas, Mechanisms of cement hydration, Cem. Concr. Res. 41 (2011) 1208–1223, https://doi.org/10.1016/J.CEMCONRES.2010.09.011.
[47] J. Shukla, V.P. Mohandas, A. Kumar, Effect of pH on the solubility of $CaSO_4{\cdot}2H_2O$ in aqueous NaCl solutions and physicochemical solution properties at 35 °C, J. Chem. Eng. Data 53 (2008) 2797–2800, https://doi.org/10.1021/je800465f.
[48] W. Ashraf, Microstructure of chemically activated of gamma-dicalcium silicate paste, Constr. Build. Mater. (2018), https://doi.org/10.1016/j.conbuildmat.2018.07.030.